Limnol. Oceanogr., 54(4), 2009, 1272–1281

Multi-decadal shoaling of the euphotic zone in the southern sector of the California Current System

Dag L. Aksnes[a,*] and Mark D. Ohman[b]

[a] Department of Biology, University of Bergen, Bergen, Norway
[b] California Current Ecosystem Long Term Ecological Research Site, Scripps Institution of Oceanography, La Jolla, California

Abstract

We document a long-term reduction in Secchi depth of 0.06–0.13 m yr^{-1} in the southern California Current System (CCS) over the period 1969–2007, reflecting a long-term shoaling of the euphotic zone. Calibrated water clarity observations from 1949 to 1954 reinforce the results indicating a progressive shoaling. For the inshore area, 150 km off the coast, Secchi disk has shoaled 8.4 ± 1.2 m since 1949. This change has been accompanied by a nitracline shoaling of 18.2 ± 6.4 m since 1969 and an increase in chlorophyll *a* since 1978. These changes have occurred despite an increase in density stratification in the CCS. Increased stratification has been linked by others to decreased nutrient fluxes, reduced primary production, increased water transparency, and a deepening of the euphotic zone, contrary to our findings. We explore this apparent paradox with a simple steady-state model of the thickness of the euphotic zone. A sensitivity analysis suggests that the observed shoaling of the euphotic zone is consistent with a doubling in nutrient upwelling, but in this analysis we also consider alternative causes for such shoaling: water-column darkening caused by freshening, increased residence time of the phototrophic biomass in the euphotic zone, and supply of nutrients of anthropogenic origin.

Increased stratification of the ocean water column is generally believed to restrict nutrient supply into the euphotic zone and cause lowered biological production (Roemmich and McGowan 1995*a*,*b*; Sarmiento et al. 2004), especially in low- to midlatitude ocean regions (Behrenfeld et al. 2006; Polovina et al. 2008). Together with increased stratification and reduced nutrient fluxes, average phytoplankton concentrations are expected to decline and the euphotic zone to deepen. Among other ocean regions, these consequences of water-column density stratification have been invoked for the California Current System (CCS) (Roemmich and McGowan 1995*a*; McGowan et al. 2003; Di Lorenzo et al. 2005), which has experienced surface-enhanced warming, slight freshening, and stronger stratification during the last 50–60 yr (Palacios et al. 2004; Kim and Miller 2007; Lavaniegos and Ohman 2007).

The long-term observations of the CCS carried out by the California Cooperative Oceanic Fisheries Investigations (CalCOFI) provide an excellent empirical foundation for testing these expectations. Begun in 1949, and continuing actively today, CalCOFI and now the associated California Current Ecosystem Long-Term Ecological Research site furnish one of the few multi-decadal, interdisciplinary ocean time series in the world ocean. Moreover, CalCOFI is a space-resolving time series: measurements are made not at a single location, but across a range of hydrographic conditions within this Eastern Boundary Current system. Among the properties measured systematically by CalCOFI is Secchi depth. Because Secchi depth and the thickness of the euphotic zone are closely related, Secchi disk observations of the CalCOFI program provide us an opportunity to test whether the euphotic zone of the CCS has deepened as expected from previous studies.

As we will show, contrary to simple expectations from the stratification hypothesis, the observations clearly suggest a long-term shoaling of the euphotic zone over the period 1949–2007. We also show that the time series of nitracline depth and chlorophyll *a* (Chl *a*) are consistent with such shoaling. We derive a simple steady-state model of the depth of the euphotic zone and explore the changes that would be required in different forcing variables to account for the observed shoaling of the euphotic zone. This analysis provides competing hypotheses for euphotic zone shoaling that are not limited to the CCS but are of relevance for aquatic systems in general.

Methods

CalCOFI data 1969–2007—Observations from the area east of longitude 124°45′W and between the latitudes 35°15′N and 30°30′N were obtained from the CalCOFI database (www.calcofi.org). This area corresponds approximately to that covered by CalCOFI sampling lines 76.7 to 93.3 (Fig. 1), which is the region that has been sampled consistently since 1984 on quarterly cruises. In addition to Secchi depth observations, we also make use of the observations of nitrate and Chl *a* that, beginning in 1984, were taken at the same stations as the Secchi depth observations. Because Secchi depth observations are restricted to daylight, our results on nitracline depth and Chl *a* also reflect daylight sampling only. This loss of temporal and spatial resolution, together with the seasonal and other sources of variation (Aksnes et al. 2007), precluded analyses of Secchi depth trends on a station basis, and the observations were grouped into three regions (Fig. 1). The observations were mapped on a latitude–longitude grid that consisted of 0.5° × 0.5°-sized geographic cells. We have previously shown that there is a distinct coast–offshore gradient in Secchi and nitracline depths (Aksnes et al. 2007), and we have defined three subareas: the inshore, transition, and offshore areas, which deviate slightly from the subareas that were applied by Kahru and

*Corresponding author: dag.aksnes@bio.uib.no

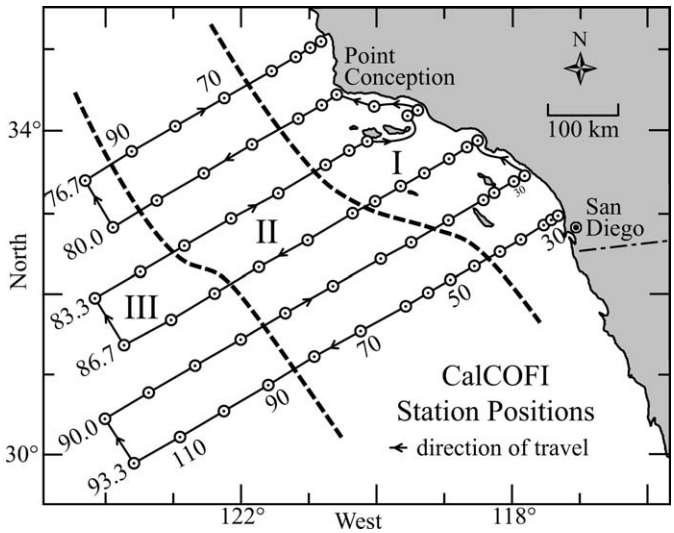

Fig. 1. CalCOFI sampling stations considered here. All observations were grouped according to their geographical position into three subareas: inshore (I), transition (II), and offshore (III). The dashed lines show the approximate border between these subareas (*see* text for details). Numerals to the left of each sampling line indicate the line number and numerals above or below the station locations indicate the station number.

Mitchell (2000). The inshore area contained the grid cells located approximately 150 km within the coast, the offshore area contained grid cells located more than approximately 450 km off the coast, and the transition area was located in between (Fig. 1).

Following Aksnes et al. (2007) the nitracline depth, Z_N, was defined as the first depth of a water column that had a nitrate concentration of 12 μmol L^{-1}. This concentration is in the lower mid range of the nitracline concentrations found in these waters, and it is within the range that was reported for the bottom of the euphotic zone by Eppley et al. (1978). It should be noted, however, that according to the results of Aksnes et al. (2007), the relationship between the thickness of the euphotic zone and the nitracline depth is nonlinear (Table 1). Linear interpolation was used to identify nitracline depths located between sampling depths (typically from 20 bottle samples per vertical profile). The

Table 1. The thickness of the euphotic zone (Z_e) compared with the nitracline depth (Z_N), defined as the depth where the nitrate concentration equals 12 μmol L^{-1}. The attenuation of downwelling irradiance (K) determines the depth of the euphotic zone according to $Z_e = 4.61/K$ (*see* Eq. 2). We have applied $Z_N = -\ln(0.039K)/K$, which was derived by Aksnes et al. (2007) for the CCS.

Light attenuation	Thickness of euphotic zone	Nitracline depth
K (m^{-1})	Z_e (m)	Z_N (m)
0.05	92	125
0.10	46	55
0.15	31	34
0.20	23	24

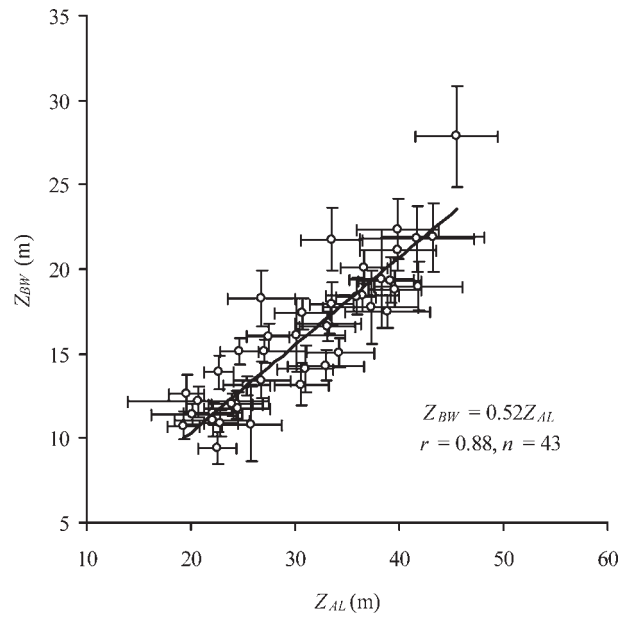

Fig. 2. Comparison between the depth of disappearance of the BW disk (Z_{BW}) and of the artificial light (Z_{AL}) that was used in the period 1949–1954. Each point represents the average depths (±SE) of a geographical cell. The size of each of the 43 geographical cells was 2° × 2°, and the cells were located from 24°N to 44°N. Each cell contained on average 18 observations for each of the two methods.

Chl *a* concentrations we report are the average concentration above the observed Secchi depth.

Water clarity observations 1949–2007—From 1969 to 2007 the Secchi depth measurements used a uniform white Secchi disk in daylight hours. Additional observations of water clarity were extracted from original CalCOFI cruise reports from the years 1949, 1950, 1951, and 1954 that were archived in the library at the Scripps Institution of Oceanography. In this earlier time period, observations were made both day and night. At night, the depth where a lowered artificial light disappeared (AL method) was noted, and by day, a disk with black and white quadrants (BW disk) was used (J. L. Reid pers. comm.). The daytime BW disk and the AL method were compared and calibrated by arranging all 1775 observations taken during 1949–1954 on a spatial grid with cell size 2° × 2° over an area extending from 24°N to 44°N and from the coast to 132°W. Grid cells with more than 5 observations for each method were used in a linear regression analysis (Fig. 2). This procedure gave 43 grid cells with a total of 822 BW disk and 712 AL observations. The regression line for the BW disc (Z_{BW}) vs. the AL method (Z_{AL}) was $Z_{BW} = 0.49Z_{AL} + 1.0$ ($r = 0.89$, $p < 10^{-5}$, $n = 43$). This regression is not statistically different from the regression line forced through zero: $Z_{BW} = 0.52Z_{AL}$ ($r = 0.88$, $p < 10^{-5}$, $n = 43$), suggesting that the observed BW disk depth was on average 52% of the AL depth. The flashlight observations were combined with the BW disk observations by applying the calibration factor 0.52. This provided a total of 1775 water clarity observations in the period 1949–1954, but because the CalCOFI program of today covers a lesser

Table 2. Comparison of the BW disk used in the period 1949–1954 with the white Secchi disc used in the period 1969–1990. The comparison is made for 6 subareas of the offshore area that were grouped according to the approximate distance from the coast (km). A linear regression analysis, $Z_S = RZ_{BW}$ (*see* Methods), where Z_S and Z_{BW} are the mean Secchi and BW disk depths of the 6 subareas, provided the calibration factor: $R = 1.54 \pm 0.03$ (±95% CI). The number of observations is given by n.

Distance from coast (km)	BW disk observations (1949–1954)			Secchi disk observations (1969–1990)		
	Mean depth (m)	SE	N	Mean depth (m)	SE	n
450–500	17.6	0.9	31	28.2	0.9	79
500–550	16.4	2.2	9	25.2	1.6	18
550–600	19.2	1.3	19	29.6	1.2	36
600–650	17.9	0.9	14	27.7	1.0	29
650–700	20.2	1.7	10	30.1	1.2	15
700–850	21.6	1.4	26	32.9	0.9	56

geographical area, only 435 of these observations were located within the area considered in the present study (Fig. 1).

Calibration of the BW disk used in 1949–1954 against the Secchi depth observations in 1969–2007—The Secchi disk depth can be expressed (Preisendorfer 1986):

$$Z_S = \frac{\ln(\tau C_0/C_T)}{c + K} = \frac{\Gamma_S}{c + K} \quad (1)$$

where τ reflects air–water transmittance effects, C_0 is the inherent contrast of the Secchi disk, C_T the human threshold contrast for the disk, and c and K are the beam attenuation and diffuse attenuation coefficients, respectively. The white Secchi disk and the BW disk have different inherent contrasts and therefore different coupling constants (Γ_S). For water columns with equal $c + K$, Eq. 1 can be applied for calibration purposes: We define $Z_{BW} = \Gamma_{BW}/(c + K)$ for the BW disk. In combination with Eq. 1 we have $R = \Gamma_S/\Gamma_{BW} = Z_S/Z_{BW}$.

In the period 1969–1990, no statistically significant temporal trend in the annual averages of the reciprocal Secchi, which is proportional to $c + K$, could be detected for the offshore area (*see* Results). By assuming invariant $c + K$ in the offshore area back to 1949, we estimated the calibration factor R. For the offshore area we had 109 water clarity observations obtained in the period 1949–1954 and 253 Secchi disc observations obtained in the period 1969–1990 (Table 2). Given the assumption of constant water clarity in the offshore area we obtained $R = 1.54 \pm 0.03$ (±95% confidence interval [CI]), and this calibration factor was used to extend the time series of the water clarity in the inshore area back to 1949.

A steady-state model of the thickness of the euphotic zone—The thickness of the euphotic zone, Z_e (m), is determined by the clarity of the water and is commonly defined as the depth where 1% of the surface photosynthetically active radiation penetrates, i.e., $0.01 = \exp(-KZ_e)$ or

$$Z_e = \frac{4.61}{K} \quad (2)$$

where K (m^{-1}) is the attenuation coefficient for downwelling irradiance (symbols used in the model derivation are given in Table 3). This attenuation is affected by several factors, of which self-shading of the phototrophic organisms is an important contributor. In addition to light, the

Table 3. List of symbols used in the derivation of the model of the thickness of the euphotic zone (Eq. 9). Note that $K = K_C$ for oceanic case I waters (Morel 1988), which means that K_C also includes the attenuation of the water itself in such waters. We have defined $K_{\text{other}} = K - K_C$, which means that a nonzero K_{other} represents a deviation from oceanic case I waters.

Symbol	Explanation	Unit
a	Nitrate uptake rate coefficient of the euphotic zone	m^2 mg N^{-1} d^{-1}
B	Phototrophic biomass of the euphotic zone	mg N m^{-2}
B_{loss}	Loss of the phototrophic biomass from the euphotic zone	mg N m^{-2} d^{-1}
C	Average Chl *a* concentration in the euphotic zone	mg Chl *a* m^{-3}
l	Phototrophic biomass loss rate (l^{-1} is the turnover time)	d^{-1}
K	Light attenuation coefficient for downwelling irradiance	m^{-1}
K_C	Light attenuation caused by chlorophyll Eq. (8)	m^{-1}
K_{other}	Light attenuation caused by other causes than chlorophyll	m^{-1}
k	Coefficient expressing the N : Chl *a* ratio	mg N (mg Chl *a*)$^{-1}$
N	Nitrate content of the euphotic zone	mg N m^{-2}
N_S	Concentration of the nutrient reservoir below the euphotic zone	mg N m^{-3}
N_{sup}	Nitrate supply to the euphotic zone	mg N m^{-2} d^{-1}
N_{hum}	N nutrient supply to the euphotic zone from human activities	mg N m^{-2} d^{-1}
w	Upwelling rate	m d^{-1}
Z_e	Euphotic depth, which is defined by $0.01 = \exp(-KZ_e)$	m

biomass of these organisms is controlled by nutrient supply, grazing, and sinking. We will include these processes, and the derivation consists of two parts: a steady-state description of the phototrophic biomass and a description of how this biomass affects the light attenuation.

In the steady-state situation, we assume that the phototrophic biomass of the euphotic zone (B, mg N m^{-2}) is determined by the supply of nitrate (N_{sup}, mg N m^{-2} d^{-1}) and the loss of biomass (B_{loss}, mg N m^{-2} d^{-1}) into and from the euphotic zone, respectively:

$$\begin{aligned} \frac{dN}{dt} &= 0 = N_{\text{sup}} - aBN \\ \frac{dB}{dt} &= 0 = aBN - B_{loss} \end{aligned} \tag{3}$$

where N is the nitrate content of the euphotic zone (mg N m^{-2}) and a (m^2 mg N^{-1} d^{-1}) is a coefficient that characterizes the nutrient uptake rate of the phototrophic biomass. N_{sup} can be categorized into those nutrients that are supplied by upwelling and those originating from other sources such as human activities (N_{hum}, mg N m^{-2} d^{-1}):

$$N_{\text{sup}} = -wN_s + N_{hum} \tag{4}$$

where w is the upwelling rate (m d^{-1}) of nutrients into the euphotic zone from the dark reservoir with nitrate concentration, N_s (mg N m^{-3}). Note that a negative w means upwelling and a positive value indicates downwelling. Biomass is lost because of sinking and mortality, but here we introduce an aggregated loss coefficient, l (d^{-1}):

$$B_{loss} = lB \tag{5}$$

The quantity l^{-1} is the nitrogen turnover time of the phototrophic biomass in the euphotic zone. Although reuse of nitrogen (i.e., regenerated production) is not explicitly accounted for, the effect of increased regeneration is increased turnover time (i.e., a decrease in l). By combining Eqs. 3–5 the phototrophic biomass of the euphotic zone is expressed:

$$B = \frac{-wN_s + N_{hum}}{l} \tag{6}$$

This biomass causes absorption and scattering of light, which affects K and consequently the thickness of the euphotic zone (Eq. 2). The attenuation coefficient K, however, is affected by factors such as particulate and dissolved substances, other than those caused by the phototrophic organisms, and also by the attenuation of the water itself. As detailed by Morel (1988), several complications arise when the average K of the euphotic zone is quantitatively attributed to the different sources of attenuation. One such complication is that the relative contribution from different substances to the total attenuation varies with euphotic depth because these substances have different wavelength-specific attenuations, e.g., the wavelength-specific attenuation of the water itself is very different from that of the pigments. These complications are not accounted for in our simplified model and we define

$$K = K_{\text{C}} + K_{\text{other}} \tag{7}$$

where K_C is the attenuation caused by the phototrophic biomass according to the empirical model that Morel (1988) estimated for oceanic case I waters. Thus K_{other} is the deviation from such water that we attribute to substances other than the phototrophic biomass. The empirical model for oceanic case I waters (Morel 1988) is

$$K_{\text{C}} = 0.121C^{0.428} \tag{8}$$

where C is the mean pigment concentration (mg m^{-3}) of the euphotic zone.

A thought experiment is considered before we finalize the derivation: consider two different water bodies where the supply and loss terms of Eq. 6, and consequently the biomass, of the two euphotic zones are equal but where K_{other} is higher in the first water body. The euphotic zone of the first water body must then be shallower than that of the second (it follows from Eqs. 2 and 7). This means that the first water body provides less vertical habitat (i.e., space) for the phototrophic biomass, and the average biomass concentration of the euphotic zone must therefore be higher here. However, this also means that K_C (Eq. 8) must be higher in the first water body, which will shoal the euphotic zone more than the elevation in K_{other} alone predicts. To quantify this interaction effect, we need the relation between the surface integrated biomass and the average concentration of the euphotic zone, which is $B = kCZ_e$, where k is a factor converting from pigment to nitrogen units. Combination with Eq. 2, 7, and 8 provides a nonlinear equation that accounts for the interaction effect:

$$\frac{K - K_{\text{other}}}{K^{0.428}} = 0.063\left(\frac{B}{k}\right)^{0.428} \tag{9a}$$

and, by insertion of Eq. 6,

$$\frac{K - K_{\text{other}}}{K^{0.428}} = 0.063\left(\frac{-wN_s + N_{hum}}{lk}\right)^{0.428} \tag{9b}$$

Note that this equation might appear dimensionally inconsistent because the empirical nature of Eq. 2. Dimensional consistency, however, is preserved by the units of the empirical constant. Because the value of K determines Z_e according to Eq. 2, Eq. 9b enables analysis of how the thickness of the euphotic zone is affected by variations in upwelled nitrate ($-wN_S$), nutrients of anthropogenic origin (N_{hum}), turnover time of the phototrophic biomass (l^{-1}), and the variation in light attenuation of substances other than the phototrophic biomass (K_{other}).

Results

Observations in the period 1969–2007—Linear regression analyses of the observations of Secchi depth and nitracline depth vs. time suggest a long-term shoaling in all three subareas (Figs. 3, 4). The estimated Secchi depth shoaling ranged from 2.3 ± 1.5 m (mean ± 95%) in the transition

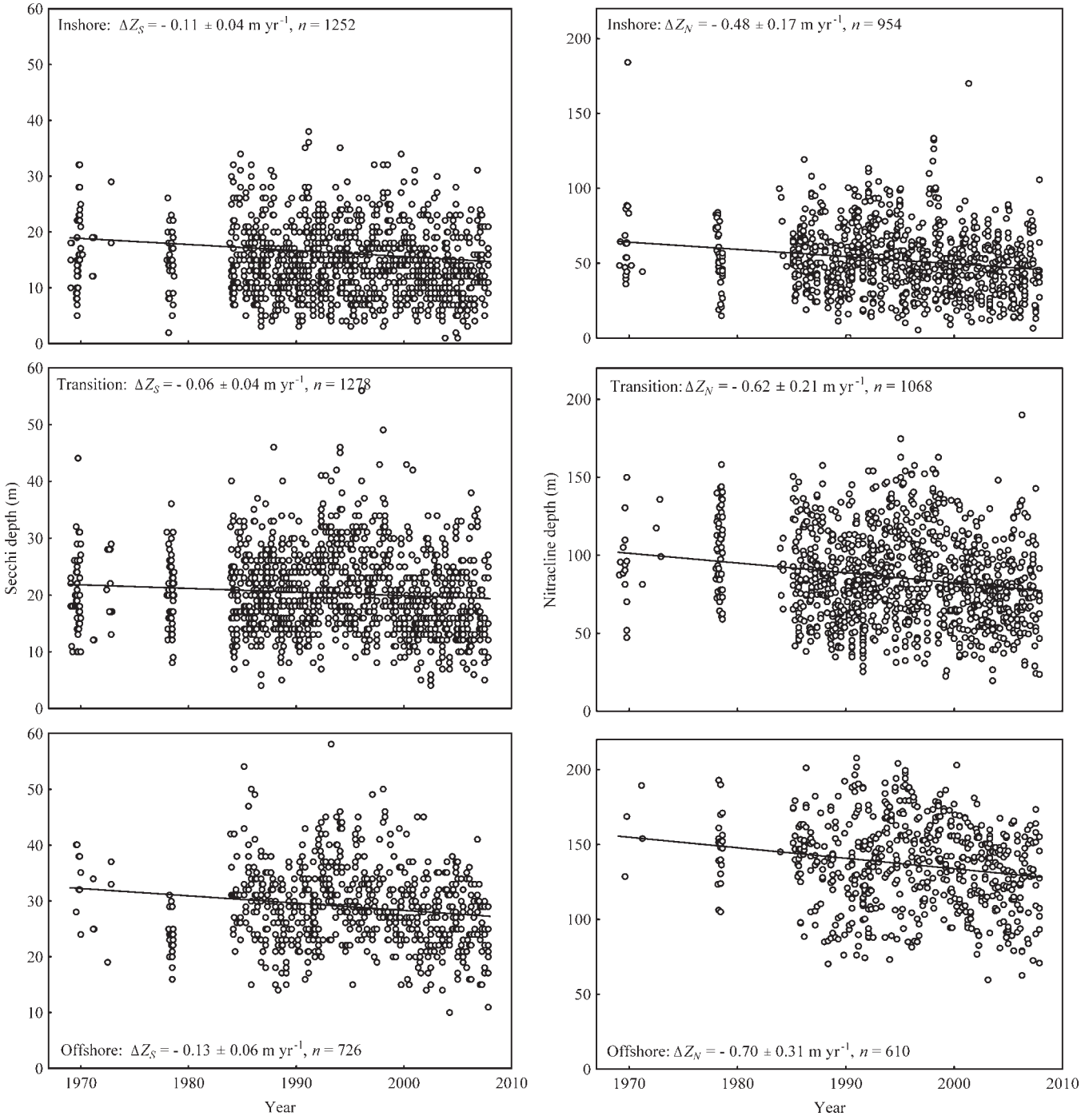

Fig. 3. Observations of Z_S (Secchi depth, left panel) and Z_N (nitracline depth, right panel) in the inshore, transition, and offshore areas of the southern sector of the CCS (*see* Fig. 1). The average annual changes (±95% confidence intervals) in the Secchi (ΔZ_S) and nitracline (ΔZ_N) depths were estimated by linear regression where n is the number of observations. For both variables in all three areas a significant ($p < 0.01$) overall shoaling (negative slopes) was measured.

area to 4.9 ± 2.3 m in the offshore area over the 38-yr period. The more pronounced nitracline depth shoaling ranged from 18.2 ± 6.5 m in the inshore area to 26.6 ± 11.8 m in the offshore area.

It might appear that the water clarity of the offshore area has been most reduced because the estimated mean shoaling rate was highest here (0.13 ± 0.06 m yr^{-1}). But the Secchi depth is inversely related to $c + K$ (Eq. 1), and changes in reciprocal Secchi depth therefore provide a more accurate picture of changes in the optical properties of the water column (Fig. 4B). Both the interannual variation and the long-term increase in reciprocal Secchi depth are higher in the inshore than in the offshore area, and this pattern is also evident in the annual variations of Chl *a* (Fig. 4D). It

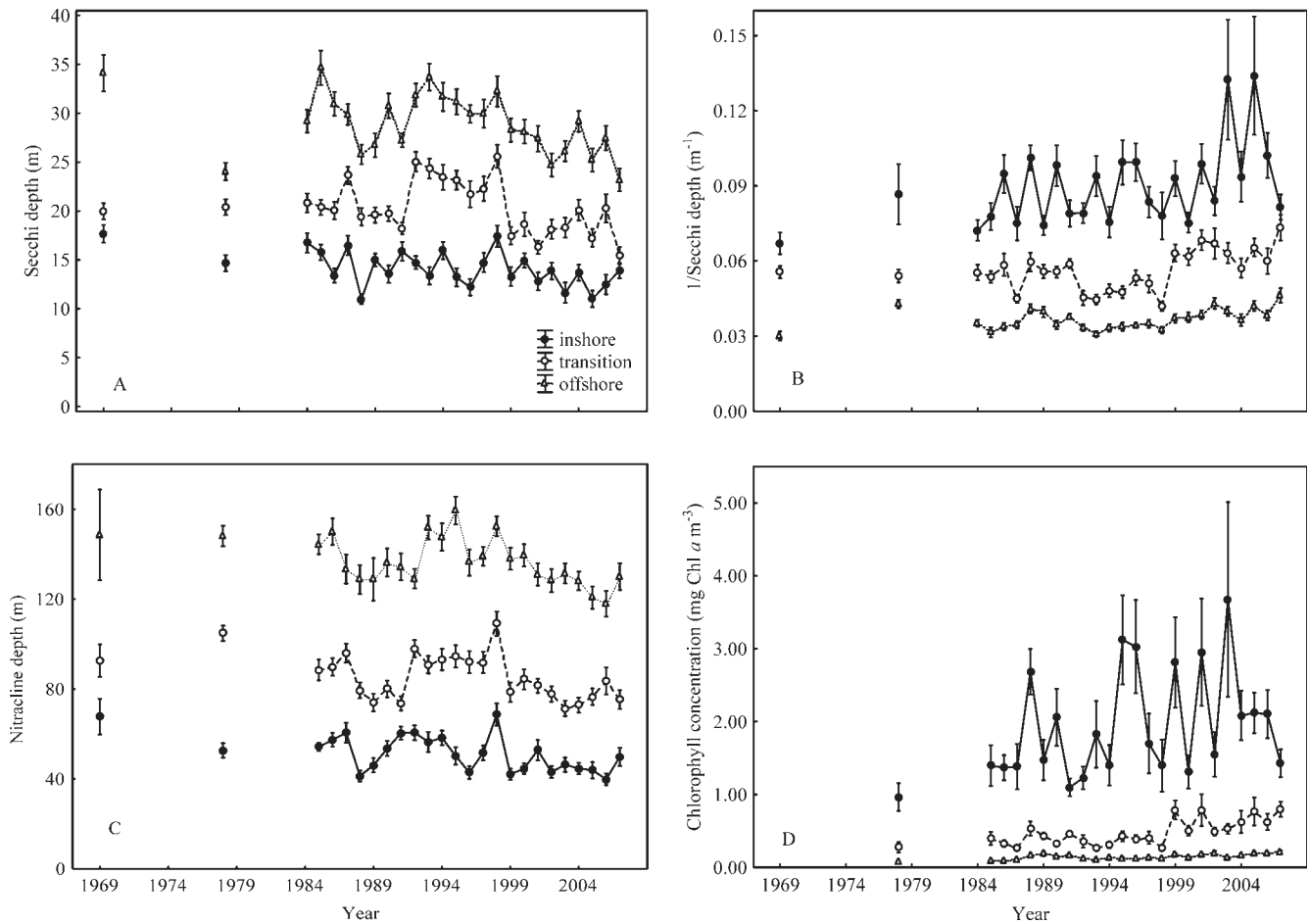

Fig. 4. Temporal changes in annual means (±SE) of (A) Secchi depth, (B) reciprocal Secchi depth, (C) nitracline depth, and (D) the Chl *a* concentration averaged for the water column above the observed Secchi depth.

can be concluded that the long-term shoaling rate of the inshore area, 0.11 ± 0.04 m yr^{-1}, which corresponds to 4.2 ± 1.5 m over the 38-yr interval, has been associated with the largest change in $c + K$.

In the period after 1978 for which Chl *a* measurements are available, the variation in Chl *a* accounted for 53% of the variation in reciprocal Secchi depth, $1/Z_S = 0.073C^{0.428}$ ($p < 10^{-5}$, $r = 0.74$, $n = 3094$) when pigment concentration was "optically" transformed according to Morel (1988), $C^{0.428}$, where C is the average Chl *a* concentration above the observed Secchi depth.

Inclusion of the calibrated water clarity observations from 1949 to 1954—These observations strengthen the picture of a long-term decrease in the water clarity in the inshore area (Fig. 5), where the estimated Secchi disk shoaling over the 58-yr period was 8.4 ± 1.2 m. The accuracy of this estimate relies on the assumption that the water clarity ($c + K$) of the offshore area was the same in 1949–1954 as in the period 1969–1990 (*see* Methods and Fig. 4B). A violation of this assumption would mean that the 8.4 m shoaling in the inshore area is an overestimate if the water clarity of the offshore area has increased (i.e., decrease in $c + K$) and an underestimate if it has decreased.

In general, self-shading of the phototrophic biomass is an important contributor to K, and the rise in Chl *a* since 1978 (Fig. 4D) suggests that this increase must have caused shoaling of the euphotic zone. This raises two questions: What has caused the increase in Chl *a*, and is this increase the only cause for the observed euphotic zone shoaling?

Sensitivity analysis—In Table 4 we have derived values for the water-column characteristics that presumably represent 1949. This set of values is consistent with Eq. 9b and serves as a 1949 baseline for the sensitivity analysis (Table 5). In this baseline we have assumed that the attenuation coefficient, K, could be described by the Morel (1988) relationship (i.e., that $K_{\text{other}} = 0$) and that upwelling was the only source of nitrate (i.e., $N_{hum} = 0$). In Table 4 we have also listed the assumed long-term changes in Secchi depth, light attenuation, euphotic depth, and Chl *a* concentration that were targeted in the sensitivity analysis. In this analysis we varied K_{other}, nitrate upwelling ($-wN_S$), and the nitrogen turnover time for the phototrophic biomass (l^{-1}) to determine the amount of variation that was needed to account for the long-term shoaling of the euphotic zone (Table 5). This analysis suggests that an elevation of 0.03 m^{-1} in the non-chlorophyll attenuation

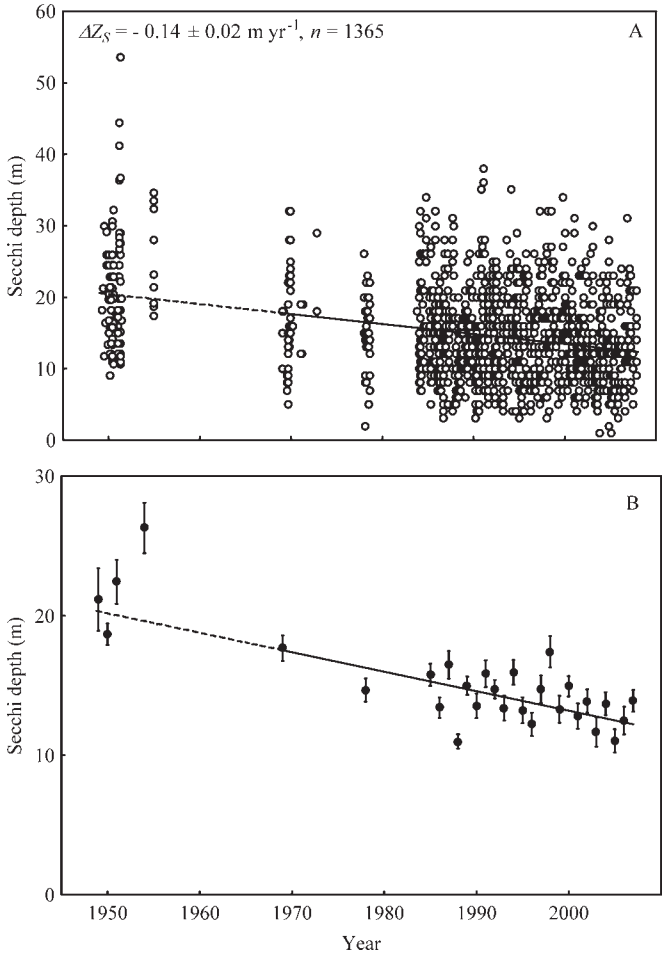

Fig. 5. (A) Secchi depth observations of the inshore area over the time period 1949–2007. Note that the observations from 1949–1954 are calibrated BW-disc observations (*see* Methods for details). The average (±SE) annual shoaling rate (ΔZ_S) was estimated with linear regression analysis where n is the number of observations. (B) Temporal changes in annual mean Secchi depth.

K_{other}, or approximately a doubling in nitrate upwelling (from 30 to 60 mg N m^{-2} d^{-1}), or a doubling in the turnover time (from 7.5 to about 14.8 d) is required to account for the 22.8 m shoaling of the euphotic zone that was assumed in Table 4. The amount of nitrogen from human sources that is required to facilitate such shoaling is N_{hum} = 30 mg N m^{-2} d^{-1}.

Discussion

Falkowski and Wilson's (1992) analysis of historical records of Secchi depth data suggests that throughout much of the central North Pacific basin, upper ocean transparency, and consequently the depth of the euphotic zone, increased slightly in the 20th century. In our study area, which is closer to the coast, the three independent observation techniques (Secchi disc, nitrate, and Chl *a* measurements) all suggest that the euphotic zone of the southern sector of the CCS has shoaled in recent decades. In terms of the reciprocal Secchi depth, this change has been most pronounced in the inshore area. In this region, which extends to about 150 km from the coast, the estimated long-term Secchi depth shoaling was 0.11 ± 0.04 m yr^{-1} for the period 1969–2007, and somewhat higher, 0.14 ± 0.02 m yr^{-1}, if the calibrated observations from 1949–1954 are included. Sanden and Håkansson (1996) have reported long-term Secchi depth shoaling for the Baltic Sea that is about 50% of our estimates, whereas the Black Sea study of Mankovsky et al. (1996) suggest a similar long-term shoaling as our study. The change reported for the Baltic Sea, however, has been associated with a larger change in reciprocal Secchi depth (and therefore in $c + K$) because the Secchi depth of this highly freshwater affected sea was initially much shallower than that of the inshore area of the CCS and also of the Black Sea.

In the same region in which we report shoaling of the euphotic zone, the hypoxic boundary has shoaled over the period 1984–2006 (Bograd et al. 2008). Bograd et al. (2008) concluded that it is unclear to what extent the decline in

Table 4. Parameter values of the sensitivity analysis for the inshore area. The 1949 baseline for the inshore area was derived according to the following assumptions: Secchi depth was estimated from the trend line in Fig. 5. The values of light attenuation, euphotic depth, and the Chl *a* concentration of the euphotic zone were obtained according to the relationships $Z_S = 1.7/K$ (Poole and Atkins 1929), $Z_e = 4.61/K$ (by definition, Eq. 2), and $K = 0.121C^{0.428}$ (Morel 1988), respectively. Eppley et al. (1979, their fig. 2) reported nitrate assimilation rates in the range 2–4 mmol m^{-2} d^{-1} for primary production over the range 0.5–1 g C m^{-2} d^{-1}. Our 1949 baseline assumes an N assimilation of 30 mg N m^{-2} d^{-1}, which corresponds to the lower end of this range. This rate was equated with nitrate upwelling ($-wN_S$) because $N_{hum} = 0$ was assumed. The value of the turnover time was obtained according to Eq. 6, i.e., $l = -wN_S/B$ where $B = kCZ_e$ and k is the N : Chl *a* ratio (assumed equal to 10). The 2007 column gives the Secchi depth predicted from the trend line in Fig. 5, whereas the other quantities were derived from the Secchi depth according to the relationships given above. The last column gives the assumed long-term change (58 yr) that was targeted in the sensitivity analysis (Table 5).

Parameter	1949 baseline	2007	Assumed change
Secchi depth, Z_S (m)	20.9	12.5	−8.4
Light attenuation, K (m^{-1})	0.081	0.136	0.055
Euphotic depth, Z_e (m)	56.7	33.9	−22.8
Chl *a*, C (mg Chl *a* m^{-3})	0.4	1.32	0.92
N : Chl a ratio, k (mg N/mg Chl *a*)	10	10	0
K_{other} (m^{-1}) (*see* text)	0	Explored in the sensitivity analysis	
N_{hum} (mg N m^{-2} d^{-1}) (*see* text)	0	Explored in the sensitivity analysis	
Nitrate upwelling, $-wN_S$ (mg N m^{-2} d^{-1})	30	Explored in the sensitivity analysis	
Turnover time, l^{-1} (d)	7.5	Explored in the sensitivity analysis	

Table 5. Sensitivity analysis for the inshore area. Sensitivity of total light attenuation (K), the depth of the euphotic zone (Z_e), the Secchi depth (Z_S), and the average Chl *a* concentration of the euphotic zone to alterations in non-chlorophyll attenuation (K_{other}), nitrogen nutrient from human activities (N_{hum}), upwelling of nitrate ($-wN_S$), and the turnover time of the phototrophic biomass (l^{-1}). Numbers in bold indicate a change from the 1949 baseline given in the first row (*see* Table 4). Each forcing parameter has been increased separately until the water characteristics of the 2007 situation (K = 0.136 m^{-1}, Z_e = 33.9 m, Z_S = 12.5 m, *Chl a* = 1.32 mg m^{-3}; *see* Table 4) have been approximated. In the case of unchanged upwelling, the last line illustrates the simultaneous change that is required in the three other forcing parameters to account for the shoaling of the euphotic zone.

Forcing parameters				Predicted characteristics of the euphotic zone (Eq. 9b)			
K_{other} (m^{-1})	N_{hum} (mg N m^{-2} d^{-1})	$-wN_S$ (mg N m^{-2} d^{-1})	l^{-1} (d)	K (m^{-1})	Z_e (m)	Z_S (m)	*Chl a* (mg Chl *a* m^{-3})
0	0	30	7.5	0.081	56.7	20.9	0.40
0.01	0	30	7.5	0.098	46.9	17.3	0.48
0.02	0	30	7.5	0.114	40.4	14.9	0.55
0.03	0	30	7.5	0.129	35.7	13.2	0.63
0.034	0	30	7.5	0.135	34.1	12.6	0.66
0	**5**	30	7.5	0.091	50.4	18.6	0.52
0	**10**	30	7.5	0.101	45.6	16.8	0.65
0	**20**	30	7.5	0.119	38.6	14.2	0.97
0	**30**	30	7.5	0.137	33.7	12.4	1.33
0	0	**35**	7.5	0.091	50.4	18.6	0.52
0	0	**40**	7.5	0.101	45.6	16.8	0.65
0	0	**50**	7.5	0.119	38.6	14.2	0.97
0	0	**60**	7.5	0.137	33.7	12.4	1.33
0	0	30	**9.0**	0.094	49.2	18.1	0.55
0	0	30	**11.0**	0.109	42.3	15.6	0.78
0	0	30	**13.0**	0.123	37.4	13.8	1.04
0	0	30	**14.8**	0.136	33.9	12.5	1.31
0.01	**5**	30	**10.5**	0.135	34.1	12.6	1.08

dissolved oxygen has been forced locally, through thermodynamic or biological processes, or remotely by advection. The increased Chl *a* documented here, which possibly is linked to increased sinking of particulate organic material, represents a potential local contributor to the observed hypoxic boundary shoaling.

The sensitivity analysis suggests that approximately a doubling of the amount of upwelled nitrate might account for the shoaling of the euphotic zone. Rykaczewski and Checkley (2008) have provided evidence that there has been a long-term increase in the wind stress curl-driven upwelling in the California Current Ecosystem over the period 1950–2006. The geographical location of this source of upwelling is largely located north of 33.5°N (fig. 3 in Rykaczewski and Checkley 2008), although it varies from year to year. If increased curl-driven upwelling were responsible for the shoaling of the euphotic zone, this should have appeared disproportionately in the northern part of our inshore area (Fig. 1). If the inshore area is subdivided into one area south and one north of 33.5°N, the estimated shoaling rate over the period 1949–2007 is indeed highest in the northern area (0.15 ± 0.03, n = 616), but it is not statistically different from that obtained in the southern area (0.12 ± 0.03, n = 749). Accordingly, although the results are consistent with a change in upwelling, we cannot exclude the possibility that factors other than increased upwelling have been responsible for the observed shoaling of the euphotic zone. The sensitivity analysis in Table 5 indicates the changes required in the non-chlorophyll attenuation, in turnover time of the phototrophic biomass (which is related to sinking and grazing), and in human nitrogen supply to account for the observed shoaling rates. Each of these potential drivers is discussed briefly below.

A trend of decreased salinity has been reported for the southern CCS and in particular in areas close to shore (Bograd and Lynn 2003; Di Lorenzo et al. 2005). Elsewhere it has been shown that salinity and light absorption are negatively correlated because of dissolved organic matter originating from land drainage (Højerslev et al. 1996). In upwelling areas like the CCS, the attenuation from pigments will normally override the effects from other attenuating substances. Our results suggest that 53% of the variation in reciprocal Secchi depth is accounted for by the Chl *a* concentration. If stations low in Chl *a* (<0.1 mg m^{-3}, altogether 314 stations) are selected, however, there is no significant relationship between the reciprocal Secchi depth and Chl *a*, but a significant negative relationship with salinity appears (Fig. 6). If the approximation $K = 1.7/Z_S$ (Poole and Atkins 1929; Idso and Gilbert 1974) is assumed, the observation in Fig. 6 suggests a decrease in the light attenuation of 0.014 m^{-1} per unit of salinity. Accordingly, a long-term freshening of the CCS, which is less than a change in salinity of 0.1 (Bograd and Lynn 2003; Di Lorenzo et al. 2005), could contribute marginally to shoaling of the euphotic zone. The sensitivity analysis suggests that K_{other} would have to increase 0.03 m^{-1} to account for the observed shoaling, which is far above the freshening effect indicated above.

In general, a change in grazing and/or sinking rate will affect the turnover time of the phototrophic biomass and

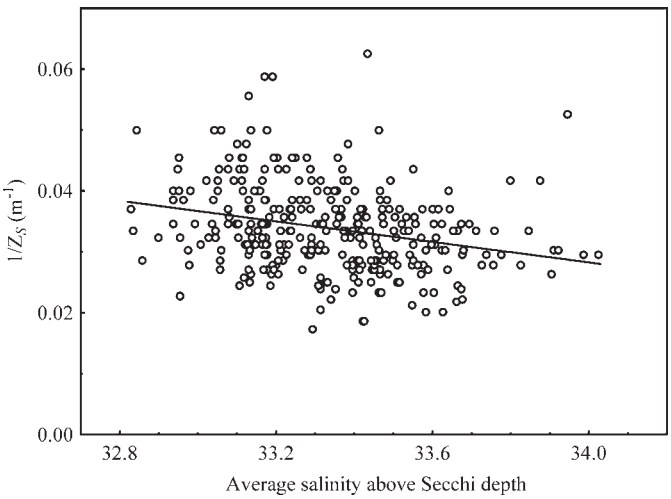

Fig. 6. Relationship between the reciprocal Secchi depth ($1/Z_S$) and salinity for the stations where average Chl *a* above Secchi depth was lower than 0.1 mg m^{-3}. The slope of the fitted regression line is -0.008 ± 0.003 m^{-1} per unit of salinity ($\pm$CI) ($p < 10^{-5}$, $n = 314$). For these low Chl *a* concentrations there was no significant relationship ($p > 0.05$) between reciprocal Secchi depth and the Chl *a* concentration.

consequently the water clarity (Table 5). A trend of reduced zooplankton biomass has been reported for the CCS (Roemmich and McGowan 1995*a*,*b*) that has now been attributed to a decrease in the salp and doliolid biomass (Lavaniegos and Ohman 2003, 2007). It can be hypothesized that reduced grazing has increased the turnover time of the phototrophic biomass. The secular increase in the density stratification (Bograd and Lynn 2003; Kim and Miller 2007; Lavaniegos and Ohman 2007) might also have affected the turnover time positively (e.g., through slower sinking). The sensitivity analysis suggests that a 50% increase in the turnover time has the same effect on euphotic shoaling as a 50% increase in upwelling. This suggests that potential effects of grazing and stratification on turnover time deserve future attention as potential mechanisms for euphotic shoaling in the CCS and elsewhere.

In some enclosed coastal seas, long-term reduction in water clarity has been connected to human-caused nutrient emissions (Mankovsky et al. 1996; Sanden and Håkansson 1996). Conversi and McGowan (1994) examined the natural vs. human-caused variability of water clarity close to the coast in the Southern California Bight with particular emphasis on sewage discharges. Although their results did not provide a totally unambiguous picture, they indicated that most of the water clarity variability was driven by bight-wide natural phenomena. The N emission from the four primary sewage treatment plants around the Southern California Bight was approximately 50×10^6 kg in 2004 (E. Stein pers. comm., Southern California Coastal Water Research Project). This corresponds to an average load of 3 mg N m^{-2} d^{-1} for the inshore area (approximately 50,000 km^2), which, according to the sensitivity analysis, might have caused a 5-m shoaling of the euphotic zone in this area. Considerably more N emission would be needed to account for the shoaling actually observed, and although there is more from other treatment plants and nonpoint discharge, it is unclear to what extent the total emitted N would be available for production in the euphotic zone. Unless the N emissions or the turnover time (7.5 d) of the phototrophic biomass are seriously underestimated, these emissions cannot account for much of the euphotic zone shoaling. Moreover, they are discharged in a restricted geographic area at the coastal boundary, and are unlikely to influence the transition or offshore regions.

One forcing variable was varied at a time in the sensitivity analysis (except in the last line of Table 5). Simultaneous changes in two or more of the forcing factors obviously require less change in each of them to account for the observed shoaling. A rise of 0.01 m^{-1} in K_{other}, a rise of 3 d in the turnover time (l^{-1}) , and an $N_{hum} = 5$ mg N m^{-2} d^{-1} are sufficient (Table 5) to account for the euphotic zone shoaling from 56.7 to 33.9 m that is indicated in Table 4. This illustrates that changes in several drivers need to be considered in future analyses of observed changes in the euphotic zone, and in particular drivers that tend to be correlated.

Our results are not consistent with previous suggestions that increased density stratification of the water column necessarily leads to decreased phytoplankton biomass and primary production in permanently stratified regions of the ocean. More than 80% of the domain studied here is permanently stratified (mean sea surface temperatures >15°C, using criteria of Behrenfeld et al. 2006), including all stations except those in the Point Conception upwelling zone in the northern portion of our region I. However, shoaling of the euphotic zone and nitracline and increased chlorophyll concentration occurred throughout the present study domain. Globally averaged primary production values inferred from satellite imagery have been interpreted as showing a downward trend between 1999 and 2006 (Behrenfeld et al. 2006), yet recent results of Kahru et al. (2009), using similar methods but calibrated against the extensive CalCOFI primary production measurements, illustrate a different trend off the west coast of North America from ~18°N to 45°N. Kahru et al. (2009) found a temporal increase in maximum primary production values and no evidence for a decline in the offshore, stratified domain. They found no relationship between primary production trends and an upwelling index, but did not differentiate wind-stress curl from coastal boundary upwelling, as did Rykaczewski and Checkley (2008). In conclusion, caution should be exercised before applying global averages to defined ocean regions, and calibrated in situ measurements are essential.

In summary, our results suggest that, contrary to previous expectations of the consequences of ocean stratification, there has been a pronounced long-term shoaling of the euphotic zone of the coastal area of the southern sector of the CCS over the period 1949–2007. Our analysis suggests that the observed shoaling in Secchi depth is consistent with a doubling in nitrate upwelling in the inshore area since 1949. It is unclear, however, whether such increase in upwelling has taken place over the same

areas as the observed shoaling. Our analysis also considers increased turnover time, freshening, and human-caused nitrogen emissions as contributors to the observed shoaling. We suggest, in particular, that in addition to vertical nutrient fluxes, the consequences of increased density stratification on the turnover time of the phototrophic biomass (i.e., through grazing and sinking) should be addressed in future studies.

Acknowledgments

This work was sponsored in part by the Leiv Eriksson Fellowship 169601 from the Norwegian Research Council (D.L.A.) and the California Current Ecosystem Long-Term Ecosystem Research supported by National Science Foundation. We thank R. Goericke for providing SST calculations and one anonymous reviewer for valuable suggestions.

References

Aksnes, D. L., M. D. Ohman, and P. Riviere. 2007. Optical effect on the nitracline in a coastal upwelling area. Limnol. Oceanogr. **52:** 1179–1187.

Behrenfeld, M. J., and others. 2006. Climate-driven trends in contemporary ocean productivity. Nature **444:** 752–755.

Bograd, S. J., C. G. Castro, E. Di Lorenzo, D. M. Palacios, H. Bailey, W. Gilly, and F. P. Chavez. 2008. Oxygen declines and the shoaling of the hypoxic boundary in the California Current. Geophys. Res. Lett. **35:** L12607, doi:10.1029/2008GL034185.

———, and R. J. Lynn. 2003. Long-term variability in the Southern California Current System. Deep-Sea Research II **50:** 2355–2370.

Conversi, A., and J. A. McGowan. 1994. Natural versus human-caused variability of water clarity in the Southern California Bight. Limnol. Oceanogr. **39:** 632–648.

Di Lorenzo, E., A. J. Miller, N. Schneider, and J. C. McWilliams. 2005. The warming of the California current system: Dynamics and ecosystem implications. J. Phys. Oceanogr. **35:** 336–362.

Eppley, R. W., E. H. Renger, and W. G. Harrison. 1979. Nitrate and phytoplankton production in southern California coastal waters. Limnol. Oceanogr. **24:** 483–494.

———, C. Sapienza, and E. H. Renger. 1978. Gradients in phytoplankton stocks and nutrients off southern California in 1974–76. Estuar. Coast. Shelf Sci. **7:** 291–301.

Falkowski, P. G., and C. Wilson. 1992. Phytoplankton productivity in the North Pacific Ocean since 1900 and implications for absorption of anthropogenic CO_2. Nature **358:** 741–743.

Højerslev, N. K., N. Holt, and T. Aarup. 1996. Optical measurements in the North Sea–Baltic Sea transition zone. On the origin of the deep water in the Kattegat. Cont. Shelf Res. **16:** 1329–1342.

Idso, S. B., and R. G. Gilbert. 1974. On the universality of the Poole and Atkins Secchi disk-light extinction equation. J. Appl. Ecol. **11:** 399–401.

Kahru, M., R. Kudela, M. Manzano-Sarabia, and B. G. Mitchell. 2009. Trends in primary production in the California Current detected with satellite data. J. Geophys. Res. **114:** C02004, doi:10.1029/2008JC004979.

———, and B. G. Mitchell. 2000. Influence of the 1997–98 El Nino on the surface chlorophyll in the California Current. Geophys. Res. Lett. **27:** 2937–2940.

Kim, H. J., and A. J. Miller. 2007. Did the thermocline deepen in the California current after the 1976/77 climate regime shift? J. Phys. Oceanogr. **37:** 1733–1739.

Lavaniegos, B. E., and M. D. Ohman. 2003. Long-term changes in pelagic tunicates of the California Current. Deep-Sea Res. II **50:** 2473–2498.

———, and ———. 2007. Coherence of long-term variations of zooplankton in two sectors of the California Current System. Prog. Oceanogr. **75:** 42–69.

Mankovsky, V. I., M. V. Solovev, and V. L. Vladimirov. 1996. Variability of the Black Sea hydrooptical parameters in 1922–1992. Okeanologiya **36:** 370–376.

McGowan, J. A., S. J. Bograd, R. J. Lynn, and A. J. Miller. 2003. The biological response to the 1977 regime shift in the California Current. Deep-Sea Res. II **50:** 2567–2582.

Morel, A. 1988. Optical modeling of the upper ocean in relation to its biogenous matter content (case I waters). J. Geophys. Res. Oceans **93:** 10749–10768.

Palacios, D. M., S. J. Bograd, R. Mendelssohn, and F. B. Schwing. 2004. Long-term and seasonal trends in stratification in the California Current, 1950–1993. J. Geophys. Res. Oceans **109:** C10016, doi:10.1029/2004JC002380.

Polovina, J. J., F. Chai, E. A. Howell, D. R. Kobayashi, L. Shi, and Y. Chao. 2008. Ecosystem dynamics at a productivity gradient: A study of the lower trophic dynamics around the northern atolls in the Hawaiian Archipelago. Prog. Oceanogr. **77:** 217–224.

Poole, H. H., and W. R. G. Atkins. 1929. Photo-electric measurements of submarine illumination throughout the year. J. Mar. Biol. Assoc. U.K. **16:** 297–324.

Preisendorfer, R. W. 1986. Secchi disk science —visual optics of natural waters. Limnol. Oceanogr. **31:** 909–926.

Roemmich, D., and J. McGowan. 1995*a*. Climatic warming and the decline of zooplankton in the California Current. Science **267:** 1324–1326.

———, and ———. 1995*b*. Sampling zooplankton: Correction. Science **268:** 352–353.

Rykaczewski, R. R., and D. M. Checkley. 2008. Influence of ocean winds on the pelagic ecosystem in upwelling regions. Proc. Natl. Acad. Sci. USA **105:** 1965–1970.

Sanden, P., and B. Håkansson. 1996. Long-term trends in Secchi depth in the Baltic Sea. Limnol. Oceanogr. **41:** 346–351.

Sarmiento, J. L., and others. 2004. Response of ocean ecosystems to climate warming. Global Biogeochem. Cycles **18:** GB3003, doi:10.1029/2003GB002134.

Associate editor: Heidi M. Sosik

Received: 06 November 2008
Accepted: 08 March 2009
Amended: 18 March 2009